# Laser-ion acceleration through controlled surface contamination

Bixue Hou, John A. Nees, Zhaohan He, George Petrov, Jack Davis et al.

Citation: Phys. Plasmas **18**, 040702 (2011); doi: 10.1063/1.3574532
View online: http://dx.doi.org/10.1063/1.3574532
View Table of Contents: http://pop.aip.org/resource/1/PHPAEN/v18/i4
Published by the AIP Publishing LLC.

# Laser-ion acceleration through controlled surface contamination

Bixue Hou,[1,a)] John A. Nees,[1] Zhaohan He,[1] George Petrov,[2] Jack Davis,[2] James H. Easter,[1] Alexander G. R. Thomas,[1] and Karl M. Krushelnick[1]
[1]*Center for Ultrafast Optical Science, University of Michigan, 2200 Bonisteel Blvd., Ann Arbor, Michigan 48109-2099, USA*
[2]*Naval Research Laboratory, Plasma Physics Division, 4555 Overlook Ave. SW, Washington, DC 20375, USA*

(Received 12 November 2010; accepted 14 March 2011; published online 28 April 2011)

In laser-plasma ion accelerators, control of target contamination layers can lead to selection of accelerated ion species and enhancement of acceleration. To demonstrate this, deuterons up to 75 keV are accelerated from an intense laser interaction with a glass target simply by placing 1 ml of heavy water inside the experimental chamber prior to pumping to generate a deuterated contamination layer on the target. Using the same technique with a deuterated-polystyrene-coated target also enhances deuteron yield by a factor of 3 to 5, while increasing the maximum energy of the generated deuterons to 140 keV. © *2011 American Institute of Physics*. [doi:10.1063/1.3574532]

The use of short pulsed lasers to accelerate ions/protons is an active research field;[1,2] one that may have many applications—such as the production of energetic neutrons.[3–7] Neutron sources have numerous applications in the fields of radiography, tomography, materials analysis, and nuclear detection and can be produced through fusion reactions between light nuclei. Focused ultraintense lasers have been used to generate megaelectron volt deuterons capable of producing neutrons via D–D fusion: $D + D \rightarrow {}^3He(0.8\,\mathrm{MeV}) + n(2.45\,\mathrm{MeV})$. Laser-driven neutron sources also exhibit small source size, which could improve imaging resolution in radiography and tomography. Also, ultrashort laser-driven neutron sources can enable time-resolved neutron measurements. Compared with large-scale neutron facilities, laser-based sources are smaller and more cost-effective.

The motivation behind the present experiments is based on the physics observed in previous attempts to accelerate ions from solid targets. In those experiments,[8] the ion signal produced from the interaction of intense laser pulses with the solid target was dominated by protons. This phenomenon is attributed to the presence of protons in the water and hydrocarbon residue[9] on the target surface. A recent theoretical and experimental study provides new details on the specific role played by the contaminants.[10] Under our experimental conditions ($10^5 \ll 10^8$ J/cm$^2$), the contaminants completely dominate the energy absorption and ion acceleration. The most likely explanation for this phenomenon is that the ions residing on the target surface are "peeled off" one layer at a time, the outermost layer being accelerated first and the inner ones shielded from the space-charge field. This peculiarity of ion acceleration favors the contaminants, as they form the outer layer of atoms on the target surface. Among the contaminants, the protons, with the highest charge-to-mass-ratio, are more readily accelerated by the laser-induced fields than the heavier ions. As a result, the acceleration of all other ions is suppressed. The use of laser prepulse,[11] target heating,[12] or ion guns[13] has enabled the removal of contaminant layers, but such techniques are often difficult to implement. Therefore, substitution of the contaminants with a desired species is a preferable means of obtaining energetic deuterons. In our research, this is tested by introduction of heavy water ($D_2O$) into the chamber to generate a new layer of $D_2O$ before irradiation.

In this letter, we report on this very simple method of controlling laser-accelerated species from solid targets. We demonstrate acceleration of deuterons up to 75 keV from the surface of borosilicate glass (*BK7*) by placing a small quantity (1 ml) of heavy water inside the experimental chamber before sealing and evacuating. The same procedure is also applied to *BK7* coated with a 2 $\mu$m-thick $C_8D_8$ (*CD*) film, yielding a threefold to fivefold increase in the accelerated deuteron flux and an increase in maximum energy from 90 to 140 keV in comparison with the same target, where heavy water is not introduced into the chamber.

The experiments are carried out on the lambda-cubed laser system[14] at the Center for Ultrafast Optical Science of the University of Michigan. Regeneratively amplified 3 mJ pulses are produced from the system at 500 Hz with 30 fs pulse duration. The *p*-polarized pulses are focused by an f/1.2 paraboloidal mirror onto various targets at an incidence angle of 51°. Optimization of a 5 cm-diameter deformable mirror prior to the parabolic mirror produces a focal spot size (measured under attenuated conditions) of $(1.5 \pm 0.2)$ $\mu$m (full width at half maximum), yielding a focal intensity of $\sim 4 \times 10^{18}$ W/cm$^2$ and a Rayleigh range of $2Z_R \approx 13$ $\mu$m. Optically polished *BK7* glass targets of 10 cm in diameter and 1 cm thick are prepared with and without a 2 $\mu$m-thick *CD* coating. The coating is applied by spinning a solution of 10 g of *CD* dissolved in 20 ml of toluene on a cleaned disc. In the experiments, undamaged target surface area is exposed with a wobble of $\pm 1$ $\mu$m to each laser shot by an $r\theta z$ translation stage. The intensity contrast ratio between the laser pulses and the amplified stimulated emission (ASE) in the nanosecond range is better than $10^8$, as determined by a fast photodiode. Third-order autocorrelation measurements indicate that there are no compressed prepulses within 100 ps of the main pulse. Consequently, the ASE intensity is

a)Electronic mail: houbx@eecs.umich.edu.

 

considered to be below the damage threshold of the glass.[15] Using the same system configuration, 500 keV protons were previously produced along the target normal direction.[8]

Ion spectra are measured with a Thomson parabola spectrometer along the target normal, which is equipped with a 50 $\mu$m metallic pinhole located 3.8 cm from the plasma. A 5 cm-long magnet pair following the pinhole provides a 1560 G magnetic field. The magnet pair is followed by a 2 cm-long electrode pair with a separation of 1 cm that provides an electric field of $(3 \pm 0.1)$ kV/cm to separate ion species. The parabolic traces of the ions are recorded on a CR39 plate located 8 cm from the exit of the electric field. The whole spectrometer is contained in a small secondary vacuum chamber, which is installed in the main target chamber. The larger chamber (40 l) is evacuated by a 250 l/min turbomolecular pump, while the spectrometer chamber is differentially pumped by a 70 l/min pump to avoid high-voltage breakdown initiated by ions generated in the high-repetition-rate laser target interaction.

We first generate energetic deuterons from a *BK7* glass target, which is installed near the laser focus. The target position ($z$) is then optimized under vacuum by maximizing the second-harmonic light emitted from the plasma at low laser fluence. Opening the chamber, 1 ml of $D_2O$ is placed on the floor of the chamber about 2 cm from the target surface. The $D_2O$ is allowed to boil away under a pressure of 15 mbar during rough pumping, after which the turbo pumps are started. Fifteen minutes of further pumping leads to a pressure of $3 \times 10^{-4}$ mbar in the main chamber. At this level, the CR39 plate in the spectrometer is exposed to the ions generated from ten shots without high voltage to record a reference signal and 100 shots with high voltage to disperse the ion species.

Figure 1(a) shows the scanned image of the developed CR39 plate. As with all images presented in this letter, these data are presented using a color lookup table applied to scanned gray values from 0 to 170. Many traces are apparent, all of which are identified from an analysis of the particle trajectories. In addition to native and contaminant ion species (H, B, C, and O ions), we clearly see a deuteron trace. Within the precision of our measurements, the traces of $^{10}B^{5+}$, $^{12}C^{6+}$, and $^{16}O^{8+}$ should overlap the deuteron trace. In order to rule out the contribution of these ions, the same experiment is repeated with a new *BK7* target without dropping $D_2O$ in the chamber (though with 83 shots). The scan from this experiment, shown in Fig. 1(b), exhibits very weak traces of $^{10}B^{5+}$ and $^{16}O^{8+}$ (not discernible in the scanned image) and no trace can be seen for the lower charge state of carbon, $^{12}C^{5+}$. Analysis of the data from the two runs shows that less than 5% contribution in the $D^+$ trace can be attributed to $^{10}B^{5+}$ and $^{16}O^{8+}$. In Fig. 1(a), the signals of $^{11}B^{4+}$ and $^{16}O^{7+}$ are weak, confirming the stated weakness in the production of $^{10}B^{5+}$ and $^{16}O^{8+}$ (particularly as $^{10}B$ is the less abundant isotope by a ratio of 1:4). The spectrum extracted from this trace is shown in blue circle in Fig. 2. This shows that deuterium ions can be accelerated without the use of a deuterated target material, producing a considerable yield up to 75 keV.

The proton trace in Fig. 1(a) is found to be much weaker than that in Fig. 1(b), while the heavier ion traces are much

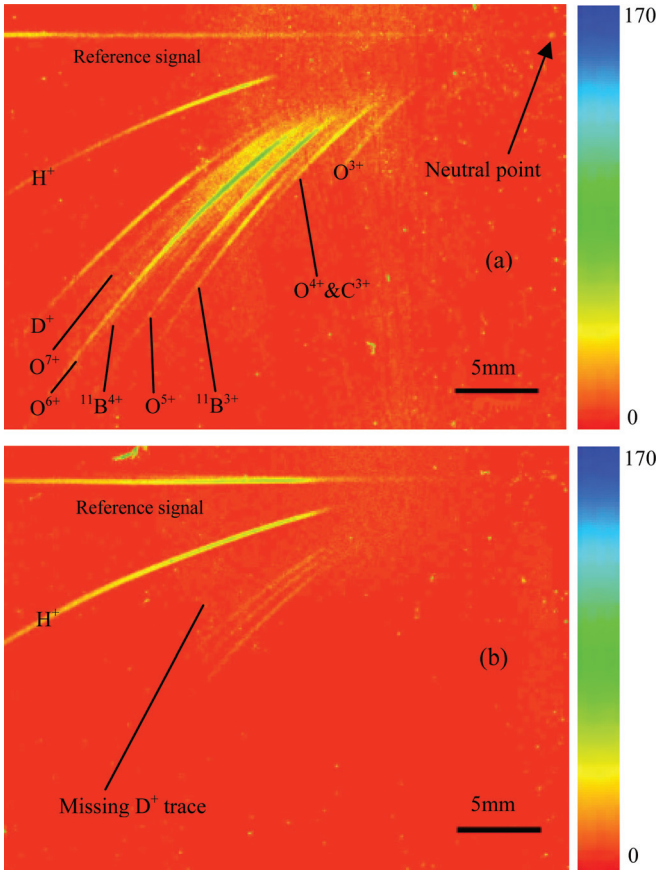


FIG. 1. (Color online) Scanned images of developed CR39 plates showing ion traces from the Thomson parabola spectrometer. Traces corresponding to the various species are identified using analytical trajectories. (a) Ions accelerated from *BK7* with $D_2O$ evaporant (100 shots) and (b) without evaporant (83 shots).

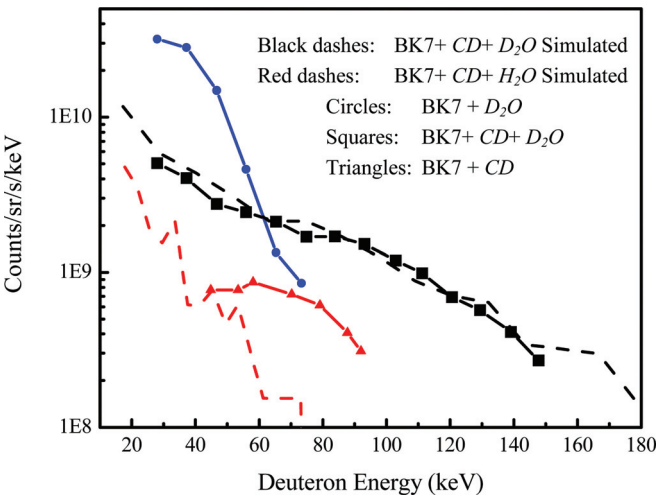


FIG. 2. (Color online) Spectra extracted from the deuteron traces in Figs. 1 and 3, and PIC simulation results. Circles (blue): from *BK7* with evaporated $D_2O$; squares (black): from 2 $\mu$m-thick deuterated polystyrene film on *BK7* with evaporated $D_2O$; triangles (red): from 2 $\mu$m-thick deuterated polystyrene film on *BK7* without evaporated $D_2O$. Black dashed line: simulated deuteron spectrum for $BK7 + CD + D_2O$; gray dashed line (red online): simulated deuteron spectrum for $BK7 + CD + H_2O$. Laser parameters in simulation: $I = 4 \times 10^{18}$ $W/cm^2$, $\lambda = 0.8$ $\mu$m, $D_{FWHM} = 1.5$ $\mu$m, $\tau_L \cong 30$ fs, $E_{laser} = 3$ mJ/pulse, $f = 500$ Hz, and incident angle $\theta = 51^\circ$.

stronger. The first observation indicates that the introduction of $D_2O$ reduces the acceleration of hydrogenic contaminants from the interaction. The second effect is a consequence of the reduction of the higher charge-to-mass-ratio species. It is also found that cleaning the glass target with $D_2O$ prior to installing it in the experimental chamber with the $D_2O$ evaporant provides only slight enhancement to the deuteron yield. The particular location of the $D_2O$ source on the target chamber floor has nearly no effect on the deuterium acceleration.

A second experiment confirms the enhancement of deuteron acceleration from a 2 $\mu$m-thick *CD* film on *BK7*, modified by evaporating $D_2O$ in the chamber. Scanned images of the developed CR39 plates are shown in Fig. 3. Figure 3(a) shows the traces of ions accelerated from a coated glass disc in the absence of $D_2O$, while Fig. 3(b) shows those generated from the same target with $D_2O$ evaporated into the chamber. The indicated deuteron signal in Fig. 3(b) is greatly enhanced. The spectra for these two cases are shown in Fig. 2 (red triangles—without $D_2O$ and black squares—with $D_2O$), where the deuteron yield is seen to increase by three to five times. In these plates, ion counts in the high-energy portions of the $D^+$ spectra are subject to some uncertainty due to signal from scattered high-atomic-number ions. However, comparing the two spectra for *CD*-coated targets in Fig. 2, the evaporation of $D_2O$ in the chamber clearly enhances the maximum deuteron energy from 90 keV (red triangles) to 140 keV (black squares). Again we see that the introduction of $D_2O$ reduces proton flux while enhancing heavier ion acceleration, including that of deuterons.

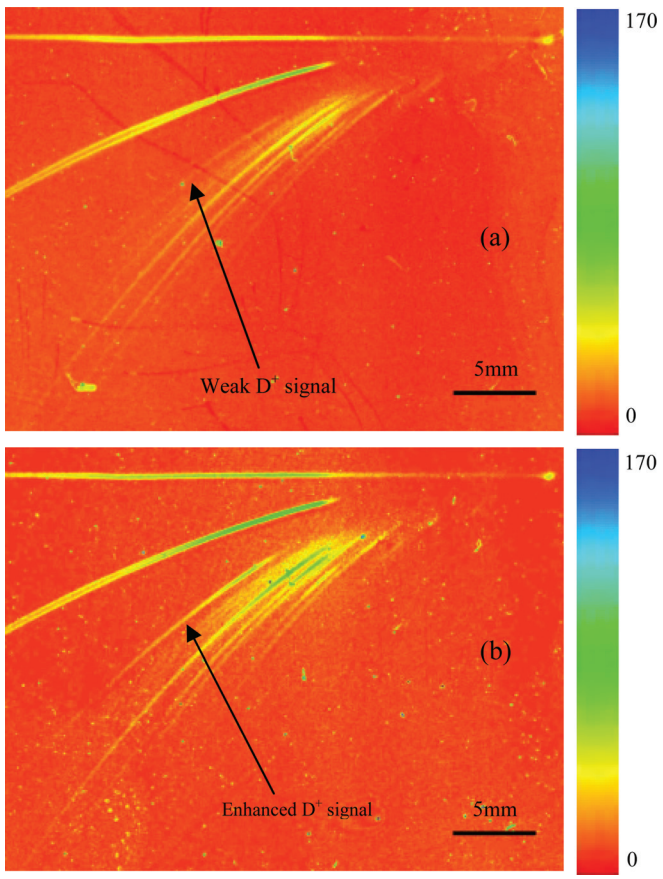


FIG. 3. (Color online) Scanned images of developed CR39 plates generated from (a) 2 $\mu$m-thick deuterated polystyrene on *BK7* and (b) the same target with 1 ml of heavy water evaporated into the chamber.

There is another interesting contrast between ion spectra taken with (black squares) and without (blue circles) a *CD* film, when $D_2O$ is added to the chamber. The introduction of the film is seen to increase energy *at the expense of* flux. This may be due to the efficacy of substituting the $D_2O$ contaminant on the surface of the different materials, as *CD* is likely to have a contaminant layer with different characteristics from one on *BK7*.

To estimate the maximum deuteron energy, we adopted the blow-off model for the expanding plasma sheath in vacuum.[16,17] The ion velocity is comparable to that of an ion's sound speed $C_h = \sqrt{T_h/M}$, with $C_h \cong 511(\sqrt{1+0.73I_{18}\lambda^2}-1)$ being the hot electron temperature in units of kilo electron volts, $I_{18}$ is the laser intensity in units of $10^{18}$ $W/cm^2$, and $M$ is the ion mass. In order to acquire full speed, the ion must traverse the plasma sheath—a length comparable to the Debye length $\lambda_D = \sqrt{T_h/(4\pi n_{\rm crit}e^2)}$ of the hot expanding electrons at the critical density $n_{\rm crit} \cong 1.3\times10^{21}{\rm cm}^{-3}$. If, however, the laser pulse duration $\tau_L$ is shorter than the time, $\tau_{\rm SW} \cong 2\lambda_D/C_h$, that it takes an ion to traverse the plasma sheath, the ion energy must be scaled approximately by the ratio $\tau_L/\tau_{\rm SW}$. A crude estimate of the maximum deuteron energy, $E^D_{\rm max} \cong (1/2){\rm MC}^2_h(\tau_L/\tau_{\rm SW}) = (1/2)T_h(\tau_L/\tau_{\rm SW})$, for $T_h = 500\,{\rm keV}$ [corresponding to $I = 4\times10^{18}\,{\rm W/cm^2}$], $C_h \cong 5\times10^8\,{\rm cm/s}$, $\lambda_D \cong 0.2\,\mu{\rm m}$, and $\tau_L \cong 30\,fs$, yields $E^D_{\rm max} \cong 100\,{\rm keV}$, agreeing well with the experimental data.

The deuteron flux $F_D = N_D f/\delta\Omega$ is estimated from the total number of accelerated deuterons per shot, $N_D \cong (1/4)\pi D^2_{\rm FWHM}L_D n_D$ emitted into a solid angle of $\delta\Omega$ and multiplied by laser repetition frequency $f$. One expects the plasma sheath to deplete a "contaminant" layer of $D_2O$ with thickness of $\sim$2 nm.[10] We assume also that the deuterons are emitted in a solid angle of $\sim$1sr (observed in simulations). With conditions relevant to our experiments ($f$ = 500 Hz, $D_{\rm FWHM} = 1.5\mu{\rm m}$, $L_D$ = 2nm, and $n_D = 6\times10^{22}{\rm cm}^{-3}$), we get $N_D \cong 2\times10^8$ deuterons/shot and deuteron flux on the order of $F_D \cong 1\times10^{11}$ deuterons/sr/s. This number is consistent with the experimental results in the case of *BK7* + *CD* + $D_2O$, plotted in Fig. 2, for which the integrated data yields $F^{\rm exp}_D \cong 2\times10^{11}$ deuterons/sr/s.

We performed 2D particle in cell (PIC) simulations with conditions matching those of the experiments (Fig. 2). The *BK7* + *CD* + $D_2O$ target was modeled as 1 $\mu$m Si + 2 $\mu$m *CD* + 2 nm $D_2O$. The width of the targets is 10 $\mu$m and the incident angle of the laser with respect to the targets is $\theta = 51°$. The laser radiation is linearly polarized and propagates in the $+x$ direction. Laser intensity profile $I(t,y) = I_0\sin^2(\pi t/\tau_0)\exp(-y^2/R_0^2)$ with parameters $I = 4\times10^{18}\,{\rm W/cm^2}$, $R_0 = 0.9\,\mu{\rm m}$, and $\tau_0 = 2\tau_L = 60\,fs$ is used. The laser pulse energy $E_{\rm laser} = \pi R_0^2 I_0 \tau_L \cong 3\,{\rm mJ}$ corresponds to that used in the experiments. The simulation box is a square with dimensions $12\times12\,\mu{\rm m}^2$, large enough to keep the particles inside during a simulation run, and the cell size is $10\times10\,{\rm nm}^2$. Particles and fields are advanced with a time step $\Delta t \cong 0.02$ fs and the total simulation time is 120 fs. The number of computational particles

is $18 \times 10^6$ with ~70 particles/cell for electrons and ~20 particles/cell for ions. The masses of electrons and ions used in the simulations are the actual ones, i.e., no scaling or artificial mass ratios between electrons and ions have been introduced. All particles, including ions, are mobile. They are initialized with velocities with random orientation corresponding to temperature 1 eV. The charges of carbon and oxygen are assumed to be four. The electron density in the bulk of the target is $\sim 150\, n_{\mathrm{crit}}$. To allow outgoing electromagnetic waves to leave the computational domain without spurious reflections from the edges, we use boundary conditions for the electric field in the form $(\partial/\partial t \pm c(\partial/\partial x))\vec{E} = 0$ propagating in the $\pm x$ direction and $(\partial/\partial t \pm c(\partial/\partial y))\vec{E} = 0$ propagating in the $\pm y$ direction.[18] The boundary conditions for particles are "open," i.e., the particles can leave the computational domain without reflection. The calculated ion spectrum (dashed line) is in excellent agreement with experimental data and is nearly independent of Si layer thickness. The *BK7* + *CD* target was simulated as 1 $\mu$m Si +2 $\mu$m *CD* + 2 nm $H_2O$, the latter being a thin (2 nm) contaminant layer of water vapor on top of the *CD* layer. The deuteron flux is about an order of magnitude lower compared to the previous case in which $D_2O$ plays the role of contaminant. The simulations show that the protons of the $H_2O$ layer strongly suppress the deuterons, both in flux and maximum energy, qualitatively in agreement with the experiments. Thus, these simulations confirm the hypothesis regarding the benefits of artificial contamination of deuterated polystyrene with $D_2O$.

The scaling of the maximum deuteron energy and conversion efficiency with laser intensity can be evaluated qualitatively by following the general dependence on the hot electron temperature $T_h$, which depends on the product $I_0\lambda_0^2$. The experiments have been performed at normalized laser intensity $I_0\lambda_0^2 \cong 2.5 \times 10^{18}\ \mathrm{Wcm}^{-2}\mu\mathrm{m}^2$, right at the onset of the relativistic regime, which starts at $I_0\lambda_0^2 \cong 1.37 \times 10^{18}\ \mathrm{Wcm}^{-2}\mu\mathrm{m}^2$. In the "low-intensity" (nonrelativistic) regime, the hot electron temperature as well as maximum deuteron energy and conversion efficiency tend to increase linearly with laser intensity. Scaling up to higher laser intensity, in the relativistic regime, they transit to a sublinear increase, as evident from the formula for $T_h$. The asymptotic scaling in the "high-intensity" (relativistic) regime is $\sim\left(I_0\lambda_0^2\right)^{1/2}$, which is roughly what is observed in the experiments and the simulations using ultrashort laser pulses.[16]

In conclusion, up to 75 keV deuterons are generated from *BK7* glass simply by placing heavy water inside the experimental chamber to introduce deuterium to the target surface. This procedure is also found to enhance the deuteron yield by three to five times from a 2 $\mu$m-thick *CD* film on *BK7*, the maximum energy of the generated deuterons also being increased. It is likely that this will provide a useful method for controlling accelerated species by evaporating liquids containing desirable elements in interaction chambers. It is possible that vapor can be introduced from a secondary chamber to enable selective contamination as well.

This work was supported by the Defense Threat Reduction Agency (DTRA), the Naval Research Laboratory (NRL), and a National Science Foundation Physics Frontier Center (FOCUS).

[1]A. Maksimchuk, S. Gu, K. Flippo, and D. Umstadter, Phys. Rev. Lett. **84**, 4108 (2000).
[2]K. Krushelnick, E. L. Clark, Z. Najmudin, M. I. K. Santala, M. Tatarakis, A. E. Dangor, V. Malka, D. Neely, R. Allott, and C. Danson, Phys. Rev. Lett. **83**, 737 (1999).
[3]F. Floux, D. Cognard, L.-G. Denoeud, G. Piar, D. Parisot, J. L. Bobin, F. Delobeau, and C. Fauquignon, Phys. Rev. E **1**, 821 (1970).
[4]G. Pretzler, A. Saemann, A. Pukhov, D. Rudolph, T. Schatz, U. Schramm, P. Thirolf, D. Habs, K. Eidmann, G. D. Tsakiris, J. Meyer-ter-Vehn, and K. J. Witte, Phys. Rev. E **58**, 1165 (1998).
[5]T. Ditmire, J. Zweiback, V. P. Yanovsky, T. E. Cowan, G. Hays, and K. B. Wharton, Nature **398**, 489 (1999).
[6]S. Lee, S. Kown, K. Lee, Y.-H Cha, D.-H. Kwon, S. Nam, K.-H. Yea, Y. W. Lee, Y. U. Jeong, Y. J. Rhee, and H. Cha, J. Korean Phys. Soc. **51**, 1695 (2007).
[7]S. Karsch, S. Dusterer, H. Schwoerer, F. Ewald, D. Habs, M. Hegelich, G. Pretzler, A. Pukhov, K. Witte, and R. Sauerbrey, Phys. Rev. Lett. **91**, 015001 (2003).
[8]B. Hou, J. Nees, J. Easter, J. Davis, G. Petrov, A. Thomas, and K. Krushelnick, Appl. Phys. Lett. **95**, 101503 (2009).
[9]S. J. Gitomer, R. D. Jones, F. Begay, A. W. Ehler, J. F. Kephart, and R. Kristal, Phys. Fluids **29**, 2679 (1986).
[10]G. M. Petrov, L. Willingale, J. Davis, Tz. Petrova, A. Maksimchuk, and K. Krushelnick, Phys. Plasmas **17**, 103111 (2010).
[11]R. Dinger, K. Rohr, and H. Weber, J. Phys. D: Appl. Phys. **17**, 1707 (1984).
[12]M. Hegelich, S. Karsch, G. Pretzler, D. Habs, K. Witte, W. Guenther, M. Allen, A. Blazevic, J. Fuchs, J. C. Gauthier, M. Geissel, P. Audebert, T. Cowan, and M. Roth, Phys. Rev. Lett. **89**, 085002 (2002).
[13]M. Allen, P. K. Patel, A. Mackinnon, D. Price, S. Wilks, and E. Morse, Phys. Rev. Lett. **93**, 265004 (2004).
[14]B. Hou, J. Easter, A. Mordovanakis, K. Krushelnick, and J. A. Nees, Opt. Express **16**, 17695 (2008).
[15]O. Efimov, S. Juodkazis, S. Matsuo, and H. Misawa, in Conference on Lasers and Electro-Optics/Quantum Electronics & Laser Science Conference (CLEO/QELS '2003), Baltimore, Maryland, 1–6 June 2003, Paper No. CWF4.
[16]P. Gibbon, *Short Pulse Laser Interaction with Matter: An Introduction* (Imperial College Press, London, 2005), p. 181.
[17]J. S. Pearlman and R. L. Morse, Phys. Rev. Lett. **40**, 1652 (1978).
[18]M. Petrov and J. Davis, Comput. Phys. Commun. **179**, 868 (2008)